J Sci Comput (2011) 47: 281–302
DOI 10.1007/s10915-010-9437-3

# Simulations of Shallow Water Equations with Finite Difference Lax-Wendroff Weighted Essentially Non-oscillatory Schemes

**Changna Lu · Jianxian Qiu**

Received: 5 July 2010 / Revised: 28 October 2010 / Accepted: 12 November 2010 /
Published online: 25 November 2010


**Abstract** In this paper we study a Lax-Wendroff-type time discretization procedure for the finite difference weighted essentially non-oscillatory (WENO) schemes to solve one-dimensional and two-dimensional shallow water equations with source terms. In order to maintain genuinely high order accuracy and suit to problems with a rapidly varying bottom topography we use WENO reconstruction not only to the flux but also to the source terms of algebraical modified shallow water equations. Extensive simulations are performed, as a result, the WENO schemes with Lax-Wendroff-type time discretization can maintain nonoscillatory properties and more cost effective than that with Runge-Kutta time discretization.

**Keywords** Lax-Wendroff-type time discretization · Weighted essentially non-oscillatory schemes · Shallow water equations · High order accuracy

## 1 Introduction

In this paper, the finite difference WENO (Weighted Essentially Non-oscillatory) schemes with Lax-Wendroff-type time discretizations are used to simulate discontinuous flows of the shallow water equations with source terms.

The research of C. Lu was supported by NSFC 40906048 and Science research fund of Nanjing University of Information Science & Technology 20090203. The research of J. Qiu was supported by NSFC 10931004.

C. Lu
College of Mathematics & Physics, Nanjing University of Information Science & Technology, Nanjing, Jiangsu 210044, P.R. China
e-mail: luchangna@nuist.edu.cn

J. Qiu (✉)
Department of Mathematics, Nanjing University, Nanjing, Jiangsu 210093, P.R. China
e-mail: jxqiu@nju.edu.cn

J. Qiu
School of Mathematical Sciences, Xiamen University, Xiamen, Fujian 361005, P.R. China
e-mail: jxqiu@ustc.edu

WENO schemes were developed from essential non-oscillatory (ENO) scheme [7], which share many advantages with and usually performed better than total variation diminishing (TVD) or total variation bounded (TVB) schemes, because they use an adaptive stencil trying to obtain information from the smoothest regions. WENO schemes use a convex combination of all candidate stencils instead of just one as in the original ENO, the first WENO scheme was constructed in [10] for the third order finite volume version in one space dimension, then the third and fifth order finite difference WENO schemes in multi-space dimensions were constructed [8], higher order WENO finite difference schemes were designed in [3]. WENO improves upon ENO in robustness, better smoothness of fluxes, better steady convergence, better provable convergence properties, and more efficiency [14]. WENO is a procedure of spatial discretization; namely, it is a procedure to approximate the spatial derivative terms. The WENO schemes are a very important class of high accuracy numerical methods, they have been developed in recent years as a class of high order finite difference or finite volume methods for hyperbolic conservation laws [8, 10], they give sharp, non-oscillatory discontinuity transitions and at the same time provide high order accurate resolutions for the smooth part of the solution, and the WENO schemes are widely used in the other application [1, 2, 17, 19]. Xing and Shu [16] designed high order finite difference WENO schemes with Runge-Kutta time discretization to shallow water equations with non-flat bottom, extensive tests are performed to verify its high order accuracy, the exact C-property, and good resolution for smooth and discontinuous solutions.

As we know, the performance of the shallow water equations without the source terms is similar to that of the compressible Euler equations in aerodynamics. A lot of shock and discontinuity capture methods that are well developed in aerodynamics can be used to solve the shallow water equations, including the cases with strong discontinuity. The straight forward treatment of the source terms can not maintain the high order accuracy. Zhou et al. [18] used the surface gradient method for the treatment of source term; Vukovic and Sopta [15] used both WENO and ENO to the combination of the flux and source term; most of the works did not keep same order accuracy for source terms with that for flux term.

For time-dependent problems, we need time accuracy as well. There are mainly two different approaches to approximate the time derivative [11]. One way is to use a high order ODE solver, such as Runge-Kutta method or multilevel type. The approach have the advantages of simplicity in concept and in coding, and it has good stability properties when the TVD-type Runge-Kutta or multi-step methods are used, however, TVD Runge-Kutta methods with positive coefficients cannot be higher than the fourth order accuracy. Another way is via the classical Lax-Wendroff procedure, which relies on converting all the time derivatives in a temporal Taylor expansion into spatial derivatives, by using partial differential equation (PDE), then discretizing the spatial derivatives, so it is also called the Taylor type. The approach can produce the same high order accuracy with a smaller effective stencil than that of the first way, and it uses more extensively the original PDE. However the formulation and coding could be quite complicated, especially for multidimensional systems. The Lax-Wendroff time discretization formula for finite volume is easier than that of the finite difference spatial discretizations. Qiu and Shu [11] developed a Lax-Wendroff time discretization procedure to solve Euler systems of compressible gas dynamics, which got the interesting conclusion of exploring a balance between reduction of cost and maintaining the non-oscillatory property by the scheme.

In this paper, the fifth order WENO finite difference schemes with the third order and the fourth order Lax-Wendroff-type time discretization are used to solve the one-dimensional and two-dimensional shallow water equations. We follow the ideas of Jiang and Shu about the WENO schemes [8], Rogers et al. [13] and Xing and Shu [16] about the balance of the

flux and the source terms of shallow water equations. This paper is organized as follows, in Sect. 2, we describe the discretization of the shallow water equations. Numerical examples are given to demonstrate the accuracy and the resolution of the constructed schemes in Sect. 3. Concluding remarks are included in Sect. 4.

## 2 Description of Numerical Model and Numerical Method

### 2.1 The Governing Equations

The two-dimensional conservative unsteady shallow water equations are

$$U_t + F(U)_x + G(U)_y = S, \tag{2.1}$$

with

$$U = [D, uD, vD]^T, \quad F(U) = [uD, u^2D + gD^2/2, uvD]^T,$$
$$G(U) = [vD, uvD, v^2D + gD^2/2]^T,$$

and the source terms

$$S = [0, -gDs_{ox}, -gDs_{oy}]^T, \tag{2.2}$$

where $D$ is the total water depth, $u$ and $v$ are the depth-averaged velocities in the $x$- and $y$-directions, respectively, $t$ is the time; $g$ is the gravitational acceleration, $s_{ox}$ and $s_{oy}$ are the bed slopes stresses, $s_{ox} = \partial b/\partial x$, $s_{oy} = \partial b/\partial y$, $b$ is the bottom function. Other terms could also be added into source terms in order to include effects such as friction on the bottom and Coriolis terms.

We write the shallow water equations in quasi-linear form as follows

$$U_t + A(U)U_x + B(U)U_y = S, \tag{2.3}$$

where

$$A(U) = \frac{\partial F}{\partial U} = \begin{pmatrix} 0 & 1 & 0 \\ c^2 - u^2 & 2u & 0 \\ -uv & v & u \end{pmatrix}, \quad B(U) = \frac{\partial G}{\partial U} = \begin{pmatrix} 0 & 0 & 1 \\ -uv & v & u \\ c^2 - v^2 & 0 & 2v \end{pmatrix},$$

and $c = \sqrt{gD}$ is the propagation speed of the shallow water wave. The eigenvalues of Jacobians $A$ and $B$ are

$$\lambda(A) = u - c, u, u + c, \quad \lambda(B) = v - c, v, v + c,$$

respectively. The corresponding left and right eigenvectors of Jacobian $A$ and $B$ are given as follows:

$$R_A = \begin{pmatrix} 1 & 0 & 1 \\ u - c & 0 & u + c \\ v & 1 & v \end{pmatrix}, \quad L_A = \begin{pmatrix} \frac{u+c}{2c} & -\frac{1}{2c} & 0 \\ -v & 0 & 1 \\ -\frac{u-c}{2c} & \frac{1}{2c} & 0 \end{pmatrix}, \tag{2.4}$$

$$R_B = \begin{pmatrix} 1 & 0 & 1 \\ u & 1 & u \\ v - c & 0 & v + c \end{pmatrix}, \quad L_B = \begin{pmatrix} \frac{v+c}{2c} & 0 & -\frac{1}{2c} \\ -u & 1 & 0 \\ -\frac{v-c}{2c} & 0 & \frac{1}{2c} \end{pmatrix}. \tag{2.5}$$

### 2.2 Description of the Fifth Order Finite Difference WENO Schemes

We solve the spacial derivative of shallow water equations using the finite difference formulation. In this section, we give a short overview for one-dimensional scalar hyperbolic conservation law as (2.6),

$$u_t + f(u)_x = 0. \tag{2.6}$$

The two-dimensional cases procedure in a dimension-by-dimension fashion, for more details, we refer to [8].

Denote $I_i = [x_{i-\frac{1}{2}}, x_{i+\frac{1}{2}}]$ be the $i$th cell, centered on $x_i$, we assume that the grid points are uniform with $\Delta x = x_{i+1} - x_i$. For a finite difference scheme, we evolve the point value $u_i$ at mesh points $x_i$ in time. The spacial derivative $f(u)_x$ is approximated by a conservative flux difference

$$f(u)_x|_{x_i} \approx \frac{1}{\Delta x}(\hat{f}_{i+\frac{1}{2}} - \hat{f}_{i-\frac{1}{2}}).$$

For a $(2r-1)$th order WENO scheme, the numerical flux $\hat{f}$ is computed through $r$ neighboring point values $f^{\pm}$ by $\hat{f} = \hat{f}^{+} + \hat{f}^{-}$. We use Lax-Friedrichs splitting as

$$f^{\pm}(u) = \frac{1}{2}(f(u) \pm \alpha u),$$

where $\alpha$ is taken as $\alpha = \max_u |f'(u)|$.

Let $f_i = f^{+}(u_i)$. For example, fifth order WENO scheme ($r = 3$), the 3 numerical fluxes are given by

$$\hat{f}^{+(0)}_{i+\frac{1}{2}} = \frac{1}{3}f_i + \frac{5}{6}f_{i+1} - \frac{1}{6}f_{i+2},$$

$$\hat{f}^{+(1)}_{i+\frac{1}{2}} = -\frac{1}{6}f_{i-1} + \frac{5}{6}f_i + \frac{1}{3}f_{i+1},$$

$$\hat{f}^{+(2)}_{i+\frac{1}{2}} = \frac{1}{3}f_{i-2} - \frac{7}{6}f_{i-1} + \frac{11}{6}f_i.$$

The next is to compute the smoothness indicators and the nonlinear weights. The $(2r-1)$th order WENO flux is a convex combination of all these $r$ numerical fluxes

$$\hat{f}^{+}_{i+\frac{1}{2}} = \sum_{m=0}^{r-1} \omega_m \hat{f}^{+(m)}_{i+\frac{1}{2}}.$$

The nonliner weights $\omega_m$ are defined in the following way:

$$\omega_m = \frac{\alpha_m}{\sum_{s=0}^{r-1}\alpha_s}, \quad \alpha_s = \frac{d_s}{(\varepsilon + \beta_s)^2},$$

here $d_s$ are the linear weights which yield $(2r-1)$th order accuracy, $\beta_s$ are the so-called "smoothness indicators", which measure the smoothness of the polynomials. $\varepsilon$ is a small positive constant used to avoid the denominator to become zero and is typically taken as $10^{-6}$. For the fifth order WENO scheme, the linear weights $d_s$ are given by

$$d_0 = \frac{3}{10}, \quad d_1 = \frac{3}{5}, \quad d_2 = \frac{1}{10},$$

and the smoothness indicators $\beta_s$ are given by

$$\beta_0 = \frac{13}{12}(f_i - 2f_{i+1} + f_{i+2})^2 + \frac{1}{4}(3f_i - 4f_{i+1} + f_{i+2})^2,$$

$$\beta_1 = \frac{13}{12}(f_{i-1} - 2f_i + f_{i+1})^2 + \frac{1}{4}(f_{i-1} - f_{i+1})^2,$$

$$\beta_2 = \frac{13}{12}(f_{i-2} - 2f_{i-1} + f_i)^2 + \frac{1}{4}(f_{i-2} - 4f_{i-1} + 3f_i)^2.$$

The reconstruction of $\hat{f}^-_{i+\frac{1}{2}}$ is mirror symmetry to that of $\hat{f}^+_{i+\frac{1}{2}}$. For the shallow water equations, we use the local characteristic decomposition, which is more robust than a component by component. The right eigenvectors and the left eigenvectors of the Jacobian $A$ and $B$ and Roe's average are needed for the local characteristic decomposition.

### 2.3 Balance of the Flux and the Source Terms

Here we adopt the ideas of Rogers et al. [13] about the balance of the flux and the source terms, they presented an algebraic technique for balancing the flux gradients and the source terms. The numerical imbalance is eradicated by reformulating the governing matrix hyperbolic system of conservation laws in terms of deviations away from an unforced but separately specified equilibrium state. Thus, balancing is achieved by the incorporation of this extra physical information and bypasses conventional numerical treatments of the imbalance.

The vector of conserved variables $U$ is given by

$$U = U^{eq} + \tilde{U}, \tag{2.7}$$

where $\tilde{U}$ is the deviation of $U$ from the equilibrium or still water value such that $\partial U^{eq}/\partial t = 0$. Actually, for still water values, the shallow water convenient properties $\zeta = u = v = 0$, and

$$U^{eq} = [h, 0, 0]^T, \quad \tilde{U} = U - U^{eq} = [\zeta, uD, vD]^T,$$

in which $\zeta$ is the free surface elevation above the still level $h + b$, $\zeta$ is still water height, $D = \zeta + h$ is the total water depth. The shallow water equations are transformed to

$$\frac{\partial \tilde{U}}{\partial t} + \frac{\partial [F(U) - F(U^{eq})]}{\partial x} + \frac{\partial [G(U) - G(U^{eq})]}{\partial y} = S - \frac{\partial (F(U^{eq}))}{\partial x} - \frac{\partial (G(U^{eq}))}{\partial y}, \tag{2.8}$$

$$\tilde{U}_t + \tilde{F}(U)_x + \tilde{G}(U)_y = \tilde{S}, \tag{2.9}$$

with

$$\tilde{U} = [\zeta, uD, vD]^T, \quad \tilde{F} = [uD, u^2D + g(\zeta^2 + 2h\zeta)/2, uvD]^T,$$

$$\tilde{G} = [vD, uvD, v^2D + g(\zeta^2 + 2h\zeta)/2]^T,$$

$$\tilde{S} = [0, -g\zeta s_{ox}, -g\zeta s_{oy}]^T. \tag{2.10}$$

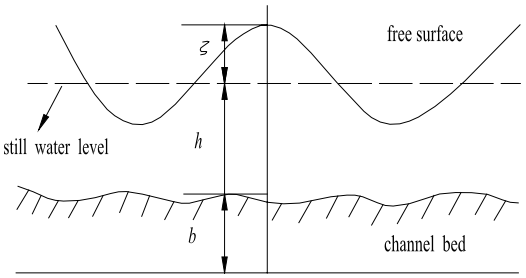


**Fig. 1** The describe of definition of variate

We can see that the Jacobian matrixes $\tilde{A}(U)$ and $\tilde{B}(U)$ of (2.9) are same as $A(U)$ and $B(U)$ of (2.1), and the discretization of (2.9) is similar to that of (2.1).

The approach taken in the paper for some examples chosen are to use the still water level as the datum $h$. It is perfectly reasonable to choose a fixed horizontal datum elsewhere as in Fig. 1, and derive the balanced hyperbolic equations using a stage-discharge approach. We denote the modified equations as usual still with

$$U_t + F(U)_x + G(U)_y = S, \tag{2.11}$$

with

$$U = [\zeta, uD, vD]^T, \quad F(U) = [uD, u^2D + g(\zeta^2 + 2h\zeta)/2, uvD]^T,$$

$$G(U) = [vD, uvD, v^2D + g(\zeta^2 + 2h\zeta)/2]^T, \quad S = [0, -g\zeta s_{ox}, -g\zeta s_{oy}]^T.$$

The scheme reduces to the original WENO scheme describe in the previous section when the bottom is flat. In order to keep the high order accuracy of the WENO scheme for shallow water equations with source terms (2.11), inspired by Xing and Shu [16], we treat source terms as follows. For two-dimensional shallow water equations, $b$ is the bottom function, we split the space derivative to $x$ and $y$ in source terms into two parts respectively as

$$S = \begin{pmatrix} 0 \\ -g\zeta s_{ox} \\ -g\zeta s_{oy} \end{pmatrix} = -\frac{1}{2}g\zeta \begin{pmatrix} 0 \\ b \\ 0 \end{pmatrix}_x - \frac{1}{2}g\zeta \begin{pmatrix} 0 \\ b \\ 0 \end{pmatrix}_x - \frac{1}{2}g\zeta \begin{pmatrix} 0 \\ 0 \\ b \end{pmatrix}_y - \frac{1}{2}g\zeta \begin{pmatrix} 0 \\ 0 \\ b \end{pmatrix}_y, \tag{2.12}$$

and perform the same WENO procedure to approximate the derivative, namely, we use the local characteristic decomposition and the same nonlinear weights to the vector $[0, b, 0]^T$ in $x$-direction and $[0, 0, b]^T$ in $y$-direction to approximate the derivative in source terms, in other words, one half of the derivative in source term is approximated by the operator obtained from the computation of $f^+$ as described in Sect. 2.2, and the other half is computed by the operator obtained from the computation of $f^-$ with biased stencils, so the approximation to source terms is also a fifth order accuracy, and the method is suit to problems with discontinuous bottom topography or the nonexistence derivative of bottom function.

### 2.4 Description of the Lax-Wendroff-type Discretization Procedure

In this section, we describe in detail the construction of Lax-Wendroff-type time discretization with WENO finite difference schemes for two-dimensional shallow water equations (2.11) [11].

Denote $\Delta t$ be the time step, $t^{n+1} = t^n + \Delta t$, we let $U^n_{i,j}$ be the approximation of the point values $U(x_i, y_j, t^n)$. For simplicity, we denote the $r$th order time derivative of $U$, namely $\frac{\partial^r U}{\partial t^r}$, by $U^{(r)}$. We also use $U'$, $U''$ and $U'''$ to denote the first, second and the third time derivatives of $U$, use $S'$, $S''$ and $S'''$ to denote the first, second and the third time derivatives of $S$, and the same to $\zeta$. In Lax-Wendroff-type time discretization procedure for the shallow water equations, the time derivatives are replaced by the spatial derivatives using the PDE [11], by a temporal Taylor expansion we obtain

$$U(x, y, t + \Delta t) = U(x, y, t) + \Delta t U' + \frac{\Delta t^2}{2} U'' + \frac{\Delta t^3}{6} U''' + \frac{\Delta t^4}{24} U^{(4)} + \cdots, \tag{2.13}$$

if we would like to obtain $k$th order accuracy in time, we would need to approximate the first $k$ time derivatives. We will proceed up to the third and the fourth order in time and fifth order in space in this paper.

First, we describe the reconstruction of the first time derivative $U' = -F(U)_x - G(U)_y + S$. In finite difference scheme for $U'_{i,j} = -F(U_{i,j})_x - G(U_{i,j})_y + S_{i,j}$, the flux vector $-F(U_{i,j})_x - G(U_{i,j})_y$ is obtained by the regular fifth order WENO finite difference procedure as described in Sect. 2.2, the two derivative in source terms $S_{i,j} = -g\zeta_{i,j}([0, b, 0]^T_x + [0, 0, b]^T_y)_{i,j}$ is computed by WENO reconstruction as described in Sect. 2.3, $\zeta_{i,j}$ is the point values of $\zeta$ at point $(x_i, y_j, t^n)$.

"Exact C-property" means that the scheme is "exact" when applied to the stationary case $D + b =$ constant and $uD = 0, vD = 0$, in other words, in the Lax-Wendroff-type time discretization with WENO schemes, $U' = U'' = U''' = \cdots = 0$ in (2.13) for any still water station. We can use the similar method of Xing and Shu [16] to prove that the upper procedure to $U'$ with WENO scheme satisfy the exact C-property and maintain the high order accuracy.

The reconstruction of the second time derivative $U'' = -(F'(U)U')_x - (G'(U)U')_y + S'$ is obtained as follow. Notice that, we will need only a one order lower flux approximation than that of the first time derivative $U'$, because of the extra $\Delta t$ factor in (2.13). Let $P_{i,j} = F'(U_{i,j})U'_{i,j}$, $Q_{i,j} = G'(U_{i,j})U'_{i,j}$, where $U_{i,j}$ and $U'_{i,j}$ are the point values of $U$ and $U'$ at the point $(x_i, y_j, t^n)$ computed above, and

$$F'(U) = A(U) = \begin{pmatrix} 0 & 1 & 0 \\ c^2 - u^2 & 2u & 0 \\ -uv & v & u \end{pmatrix}, \quad G'(U) = B(U) = \begin{pmatrix} 0 & 0 & 1 \\ -uv & v & u \\ c^2 - v^2 & 0 & 2v \end{pmatrix}. \tag{2.14}$$

We use the following the fourth order central difference approximation to get the fifth order approximation in space:

$$\begin{aligned} U''_{i,j} \approx & -\frac{1}{12\Delta x}(P_{i-2,j} - 8P_{i-1,j} + 8P_{i+1,j} - P_{i+2,j}) - \frac{1}{12\Delta y}(Q_{i,j-2} - 8Q_{i,j-1} \\ & + 8Q_{i,j+1} - Q_{i,j+2}) + S'_{i,j}. \end{aligned} \tag{2.15}$$

We assume the bottom topography is unchanged, the space derivative $[0, b_x, b_y]^T_{i,j}$ in source terms $S'_{i,j} = -g\zeta'_{i,j}[0, b_x, b_y]^T_{i,j}$ is computed by WENO reconstruction, which have been computed in the first time derivative $U'$; $\zeta'_{i,j}$, which is time derivative of $\zeta$, is the point values of $\zeta'$ at point $(x_i, y_j, t^n)$ computed above.

Notice that this approximation is conservative; namely, it can be written as a flux difference form. It seems that a more costly WENO approximation is not needed here to control spurious oscillations, presumably because this term is multiplied by an extra $\Delta t$ anyway.

In order to explain the procedure of $U''$ satisfy the exact property, we firstly consider the situation when approximation is used to $U''$ without central difference. When computing $U''$ at $(x_i, y_j)$, $F'(U)$ in $P_{i,j}$, which is the Jacobian $A(U)$ at $(x_i, y_j)$, is fixed. Therefore, C-property still holds to $P_{i,j}$, with $U'_{i,j}$ is proved to have the attribute in the first time derivative above. The same theory suit to $Q_{i,j}$. The fourth order central difference as (2.15) is a linear operator, and the coefficients are constant, so the theory will go through. For the still water station, the effect of $S'_{i,j}$ towards the approximation of $U''$ is zero because of the fact that $\zeta = \text{constant}$. So we can prove that the WENO-LW scheme maintains exactly C-property to $U''$.

The reconstruction of the third time derivative

$$U''' = -\big(F'(U)U'' + F''(U)(U')^2\big)_x - \big(G'(U)U'' + G''(U)(U')^2\big)_y + S'',$$

is obtained as follows. Let

$$P_{i,j} = F'(U_{i,j})U''_{i,j} + F''(U_{i,j})(U'_{i,j})^2, \quad Q_{i,j} = G'(U_{i,j})U''_{i,j} + G''(U_{i,j})(U'_{i,j})^2,$$

in which

$$F''(U) = A'(U) = \left(\begin{array}{ccc|ccc|ccc} 0 & 0 & 0 & 0 & 0 & 0 & 0 & 0 & 0 \\ g+2u^2/D & -2u/D & 0 & -2u/D & 2/D & 0 & 0 & 0 & 0 \\ 2uv/D & -v/D & -u/D & -v/D & 0 & 1/D & -u/D & 1/D & 0 \end{array}\right), \tag{2.16}$$

$$G''(U) = B'(U) = \left(\begin{array}{ccc|ccc|ccc} 0 & 0 & 0 & 0 & 0 & 0 & 0 & 0 & 0 \\ 2uv/D & -v/D & -u/D & -v/D & 0 & 1/D & -u/D & 1/D & 0 \\ g+2v^2/D & 0 & -2v/D & 0 & 0 & 0 & -2v/D & 0 & 2/D \end{array}\right). \tag{2.17}$$

If we denote $F''(U) = (F_1, F_2, F_3)$, where $F_1, F_2, F_2$ are the three $3 \times 3$ matrixes as above, $F''(U)(U')^2 = (F_1U', F_2U', F_3U')U'$, which also is a $3 \times 1$ vector.

Because of the extra $\Delta t^2$, we need only the third order flux approximation to get the fifth order approximation of $U'''$, we would like to use the same differences as above in space which are all of even order

$$\begin{aligned} U'''_{i,j} \approx & -\frac{1}{12\Delta x}(P_{i-2,j} - 8P_{i-1,j} + 8P_{i+1,j} - P_{i+2,j}) - \frac{1}{12\Delta y}(Q_{i,j-2} - 8Q_{i,j-1} \\ & + 8Q_{i,j+1} - Q_{i,j+2}) + S''_{i,j}. \end{aligned} \tag{2.18}$$

The space derivative $[0, b_x, b_y]^T_{i,j}$ in source terms $S''_{i,j} = -g\zeta''_{i,j}[0, b_x, b_y]^T_{i,j}$ use the computed value as above; $\zeta''_{i,j}$, which is the second time derivative of $\zeta$, is the point values of $\zeta''$ at point $(x_i, y_j, t^n)$ computed above.

The reconstruction of the fourth time derivative

$$\begin{aligned} U^{(4)} = & -(F'(U)U''' + 3F''(U)U'U'' + F'''(U)(U')^3)_x - (G'(U)U''' + 3G''(U)U'U'' \\ & + G'''(U)(U')^3)_y + S''', \end{aligned}$$

is obtained in a similar fashion. Let

$$P_{i,j} = F'(U_{i,j})U'''_{i,j} + 3F''(U_{i,j})U'_{i,j}U''_{i,j} + F'''(U_{i,j})(U'_{i,j})^3,$$

$$Q_{i,j} = G'(U_{i,j})U'''_{i,j} + 3G''(U_{i,j})U'_{i,j}U''_{i,j} + G'''(U_{i,j})(U'_{i,j})^3,$$

where

$$F'''(U) = A''(U) = (A_1, A_2, A_3), \quad G'''(U) = B''(U) = (B_1, B_2, B_3),$$

with

$$A_1(U) = \left(\begin{array}{ccc|ccc|ccc} 0 & 0 & 0 & 0 & 0 & 0 & 0 & 0 & 0 \\ -6u^2/D^2 & 4u/D^2 & 0 & 4u/D^2 & -2/D^2 & 0 & 0 & 0 & 0 \\ -6uv/D^2 & 2v/D^2 & 2u/D^2 & 2v/D^2 & 0 & -1/D^2 & 2u/D^2 & -1/D^2 & 0 \end{array}\right), \tag{2.19}$$

$$A_2(U) = \left(\begin{array}{ccc|ccc|ccc} 0 & 0 & 0 & 0 & 0 & 0 & 0 & 0 & 0 \\ 4u/D^2 & -2/D^2 & 0 & -2/D^2 & 0 & 0 & 0 & 0 & 0 \\ 2v/D^2 & 0 & -1/D^2 & 0 & 0 & 0 & -1/D^2 & 0 & 0 \end{array}\right), \tag{2.20}$$

$$A_3(U) = \left(\begin{array}{ccc|ccc|ccc} 0 & 0 & 0 & 0 & 0 & 0 & 0 & 0 & 0 \\ 0 & 0 & 0 & 0 & 0 & 0 & 0 & 0 & 0 \\ 2u/D^2 & -1/D^2 & 0 & -1/D^2 & 0 & 0 & 0 & 0 & 0 \end{array}\right), \tag{2.21}$$

$$B_1(U) = \left(\begin{array}{ccc|ccc|ccc} 0 & 0 & 0 & 0 & 0 & 0 & 0 & 0 & 0 \\ -6uv/D^2 & 2v/D^2 & 2u/D^2 & 2v/D^2 & 0 & -1/D^2 & 2u/D^2 & -1/D^2 & 0 \\ -6v^2/D^2 & 0 & 4v/D^2 & 0 & 0 & 0 & 4v/D^2 & 0 & -2/D^2 \end{array}\right), \tag{2.22}$$

$$B_2(U) = \left(\begin{array}{ccc|ccc|ccc} 0 & 0 & 0 & 0 & 0 & 0 & 0 & 0 & 0 \\ 2v/D^2 & 0 & -1/D^2 & 0 & 0 & 0 & -1/D^2 & 0 & 0 \\ 0 & 0 & 0 & 0 & 0 & 0 & 0 & 0 & 0 \end{array}\right), \tag{2.23}$$

$$B_3(U) = \left(\begin{array}{ccc|ccc|ccc} 0 & 0 & 0 & 0 & 0 & 0 & 0 & 0 & 0 \\ 2u/D^2 & -1/D^2 & 0 & -1/D^2 & 0 & 0 & 0 & 0 & 0 \\ 4v/D^2 & 0 & -2/D^2 & 0 & 0 & 0 & -2/D^2 & 0 & 0 \end{array}\right). \tag{2.24}$$

In order to get a fifth order scheme, we need to use only the second order central difference approximation to flux in $U^{(4)}$ at the point $(x_i, y_j, t^n)$, because the extra $\Delta t^3$ factor. We use the following second order approximation:

$$U^{(4)}_{i,j} \approx -\frac{1}{2\Delta x}(P_{i+1,j} - P_{i-1,j}) - \frac{1}{2\Delta y}(Q_{i+1,j} - Q_{i-1,j}) + S'''_{i,j}, \tag{2.25}$$

which is again a conservative approximation. The space derivative $[0, b_x, b_y]^T_{i,j}$ in source terms $S'''_{i,j} = -g\zeta'''_{i,j}[0, b_x, b_y]^T_{i,j}$ is computed in same fashion as above; $\zeta'''_{i,j}$, which is the third time derivative of $\zeta$, is the point values of $\zeta'''$ at point $(x_i, y_j, t^n)$ computed above.

If we require higher order accuracy in time, this procedure can be continued in a similar fashion. The exact C-property can be proved to $U'''', U^{(4)}, \ldots$ using the similar idea in $U''$. So the WENO-LW scheme maintain the exact C-property.

In the following we denote the schemes with $(2r-1)$th order WENO scheme in space and $k$th order Lax-Wendroff-type method in time as WENO$(2r-1)$-LW$k$. We will concentrate attention on WENO5-LW3 and WENO5-LW4. As a comparison by the third and the fourth order Runge-Kutta methods with WENO schemes as WENO5-RK3 and WENO5-RK4.

## 3 Numerical Results

In this section, we perform numerical experiments to test the performance of the finite difference WENO5-LW schemes developed in the previous section for shallow water equations, and compare them with the finite difference WENO5-RK schemes, addressing on the important issue of CPU time and relevant efficiency, both one-dimensional and two-dimensional shallow water equations are studied.

For CPU time comparison, all the computations are performed on a personal computer, Core (TM) 2 Duo CPU P8600 @ 2.4 GHz with 4 GB ram. In our numerical experiments, the gravitation constant is taken as 9.812 m/s$^2$. The biggest CFL numbers for WENO5-LW and WENO5-RK are about 0.51 and 1, respectively, which are obtained from standard Fourier analysis of WENO scheme with linear weights for scalar linear equation. We use 0.4 for WENO5-LW and 0.8 for WENO-RK in this paper, which are about 80% of the biggest numbers. The small positive constant in the WENO weight formula is taken as $\varepsilon = 10^{-6}$, except for the special test. Uniform meshes are used.

*Example 3.1* Test for the exact C-property. In this test case [12, 16], the bottom is defined with

$$b(x) = 5\exp\left(-\frac{2}{5}(x-5)^2\right) \quad x \in [0, 10].$$

The initial water height is defined as $D(x) = 10 - b(x)$, and the initial velocity is defined as zero. The surface should remain flat. The terminal time is taken as $t = 0.5$ s.

We take the still level $h$ as $h = 10 - b(x)$. In Tables 1, 2, $L^1$ and $L^\infty$ are errors of water height $D$ and the discharge $Du$ for WENO5-LW3 and WENO5-LW4 respectively. The results obviously confirm the theoretical result of the proposition basically. The accuracy is good.

*Example 3.2* An one-dimensional accuracy test over a sinusoidal hump [4, 10]. In order to get fifth order in accuracy test with smooth solution for WENO5-LW$k$ scheme, we do not

**Table 1** $L^1$ and $L^\infty$ errors for the accuracy for the stationary solution, WENO5-LW3 and WENO5-RK3 using $N$ space points

| $N$ | WENO5-LW3 | | | | WENO5-RK3 | | | |
|---|---|---|---|---|---|---|---|---|
| | $D$ | | $Du$ | | $D$ | | $Du$ | |
| | $L^1$ | $L^\infty$ | $L^1$ | $L^\infty$ | $L^1$ | $L^\infty$ | $L^1$ | $L^\infty$ |
| 500 | 3.28E−15 | 7.11E−15 | 1.86E−14 | 6.00E−14 | 8.67E−16 | 3.55E−15 | 6.14E−15 | 2.04E−14 |
| 200 | 9.68E−16 | 7.11E−15 | 1.29E−14 | 4.23E−14 | 6.66E−16 | 1.78E−15 | 9.38E−15 | 2.13E−14 |
| 20 | 1.87E−15 | 5.33E−15 | 1.50E−14 | 4.94E−14 | 4.09E−15 | 1.42E−14 | 3.82E−14 | 1.31E−13 |

use the regular adaptive time step $\triangle t^n = CFL \cdot \frac{\triangle x}{\max_i(|u_i^n| + \sqrt{gD_i^n})}$ for one-dimensional shallow water equations, but $\triangle t^n = CFL \cdot \frac{(\triangle x)^{\frac{5}{k}}}{\max_i(|u_i^n| + \sqrt{gD_i^n})}$.

To check the order accuracy of the schemes for a smooth solution of one-dimensional shallow water equations, we use the same test as Xing and Shu [16]. In the domain [0, 1], the bottom topography

$$b(x) = \sin^2(2\pi x),$$

the initial data are given by:

$$D(x,0) = 5 + e^{\cos(2\pi x)},$$

$$(Du)(x,0) = \sin(\cos(2\pi x)).$$

We take the still water height $h$ as $h = 5 - b(x)$. We compute up to time $t = 0.1$ s when there is no shocks in the solution, with a 2-periodic boundary conditions. The reference solution is computed with the same scheme and 25600 points, since the exact solution is unknown.

In Table 3, the $L^\infty$ numerical errors and orders of accuracy by WENO5-LW4 of water depth $D$ and the discharge $Du$ are displayed, $N$ is the number of points. For comparison, $L^\infty$ numerical errors and orders of accuracy by WENO5-RK4 schemes are also shown in

**Table 2** $L^1$ and $L^\infty$ errors for the accuracy for the stationary solution, WENO5-LW4 and WENO5-RK4 using $N$ space points

| $N$ | WENO5-LW4 | | | | WENO5-RK4 | | | |
|---|---|---|---|---|---|---|---|---|
| | $D$ | | $Du$ | | $D$ | | $Du$ | |
| | $L^1$ | $L^\infty$ | $L^1$ | $L^\infty$ | $L^1$ | $L^\infty$ | $L^1$ | $L^\infty$ |
| 500 | 1.46E−15 | 7.11E−15 | 1.15E−14 | 5.06E−14 | 4.62E−17 | 1.78E−15 | 4.10E−15 | 2.25E−14 |
| 200 | 1.01E−15 | 5.33E−15 | 1.12E−14 | 4.62E−14 | 6.22E−17 | 1.78E−15 | 3.13E−15 | 1.23E−14 |
| 20 | 1.78E−15 | 5.33E−15 | 1.64E−14 | 4.87E−14 | 3.91E−15 | 1.24E−14 | 3.36E−14 | 1.23E−13 |

**Table 3** $L^\infty$ errors and numerical orders of accuracy for the one-dimensional order test, WENO5-LW4 and WENO5-RK4 using $N$ space points

| $N$ | WENO5-LW4 | | | | WENO5-RK4 | | | |
|---|---|---|---|---|---|---|---|---|
| | $D$ | | $Du$ | | $D$ | | $Du$ | |
| | $L^\infty$ error | order | $L^\infty$ error | order | $L^\infty$ error | order | $L^\infty$ error | order |
| 25 | 7.165E−2 | | 6.060E−1 | | 7.038E−2 | | 6.257E−1 | |
| 50 | 1.672E−2 | 2.10 | 1.612E−1 | 1.91 | 1.744E−2 | 2.01 | 1.685E−1 | 1.89 |
| 100 | 4.140E−3 | 2.01 | 3.516E−2 | 2.20 | 4.323E−3 | 2.01 | 3.664E−2 | 2.20 |
| 200 | 4.943E−4 | 3.07 | 4.566E−3 | 2.95 | 5.149E−4 | 3.07 | 4.745E−3 | 2.95 |
| 400 | 2.771E−5 | 4.16 | 2.455E−4 | 4.22 | 2.885E−5 | 4.16 | 2.555E−4 | 4.22 |
| 800 | 9.966E−7 | 4.80 | 8.496E−6 | 4.86 | 1.034E−6 | 4.80 | 8.786E−6 | 4.86 |
| 1600 | 3.196E−8 | 4.97 | 2.705E−7 | 4.97 | 3.256E−8 | 4.99 | 2.763E−7 | 4.99 |

**Table 4** $L^1$ errors and numerical orders of accuracy for the one-dimensional order test, WENO5-LW4 and WENO5-RK4 using $N$ space points

| $N$ | WENO5-LW4 | | | | WENO5-RK4 | | | |
|---|---|---|---|---|---|---|---|---|
| | $D$ | | $Du$ | | $D$ | | $Du$ | |
| | $L^1$ error | order | $L^1$ error | order | $L^1$ error | order | $L^1$ error | order |
| 25 | 1.511E−2 | | 1.202E−1 | | 1.458E−2 | | 1.180E−1 | |
| 50 | 2.071E−3 | 2.87 | 2.168E−2 | 2.47 | 2.093E−3 | 2.80 | 2.220E−2 | 2.41 |
| 100 | 3.150E−4 | 2.72 | 2.827E−3 | 2.94 | 3.287E−4 | 2.67 | 2.936E−3 | 2.92 |
| 200 | 2.207E−5 | 3.84 | 1.935E−4 | 3.87 | 2.308E−5 | 3.83 | 2.022E−4 | 3.86 |
| 400 | 8.982E−7 | 4.62 | 7.768E−6 | 4.64 | 9.350E−7 | 4.63 | 8.085E−6 | 4.64 |
| 800 | 3.108E−8 | 4.85 | 2.674E−7 | 4.86 | 3.207E−8 | 4.87 | 2.759E−7 | 4.87 |
| 1600 | 1.021E−9 | 4.93 | 8.809E−9 | 4.92 | 1.040E−9 | 4.95 | 8.968E−9 | 4.94 |

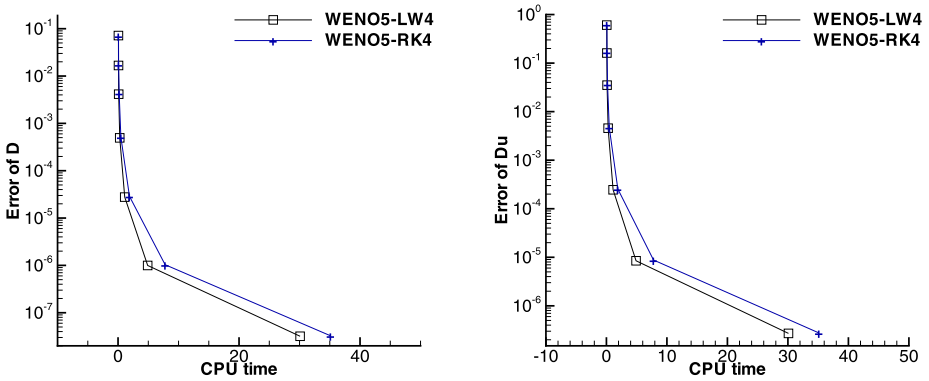


**Fig. 2** $L^\infty$ errors and CPU time for the one-dimensional order test. *Left*: water depth. *Right*: discharge

Table 3. The $L^1$ numerical errors and orders of accuracy by WENO5-LW4 and WENO5-RK4 are shown in Table 4. We can see that fifth order accuracy are almost achieved for the finite difference both WENO5-LW4 and WENO5-RK4 schemes, they produce similar numerical errors and orders of accuracy. WENO5-LW3 and WENO5-RK3 also get fifth order and nearly numerical errors, we do not list the data to save space.

In Fig. 2, we give the $L^\infty$ numerical errors and cost CPU time for $D$ and $Du$ when cell numbers are '50, 100, 200, 400, 800, 1600', and Log scale for numerical errors, we can see that the line of WENO5-LW4 always at the bottom of the line of WENO5-RK4, which means to get the same numerical error, WENO5-RK4 cost more CPU time.

*Example 3.3* Dam break on a flat bed. The dam-break problem is the most common test to evaluate the performance of shock capturing schemes in shallow flows, such as [12]. The bottom is flat $b(x) = 0$ and the initial conditions are taken as:

$$D(x,0) = \begin{cases} D_1 & x < 0 \\ D_2 & x \geq 0 \end{cases}, \quad (Du)(x,0) = 0. \tag{3.1}$$

We take the computational domain as $[-1, 1]$, $D_1 = 1$ m and $D_2 = 0.1$ m. The simulation is performed up to time $t = 0.1$ s.

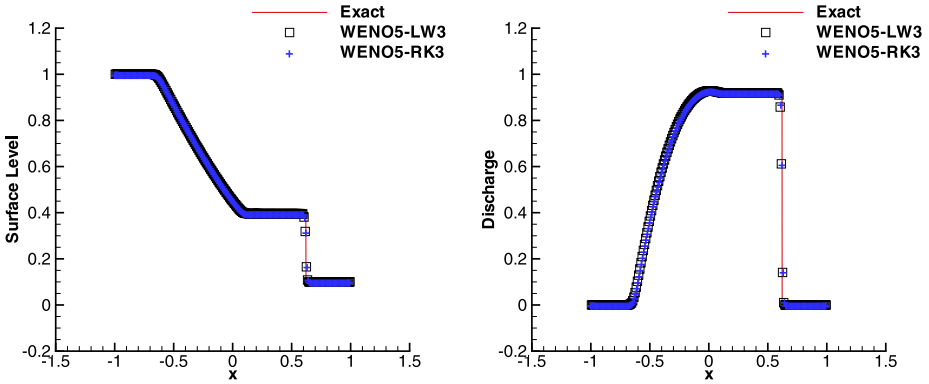


**Fig. 3** Dam break on a flat bed by WENO5-LW3 and WENO5-RK3. *Left*: water depth. *Right*: discharge

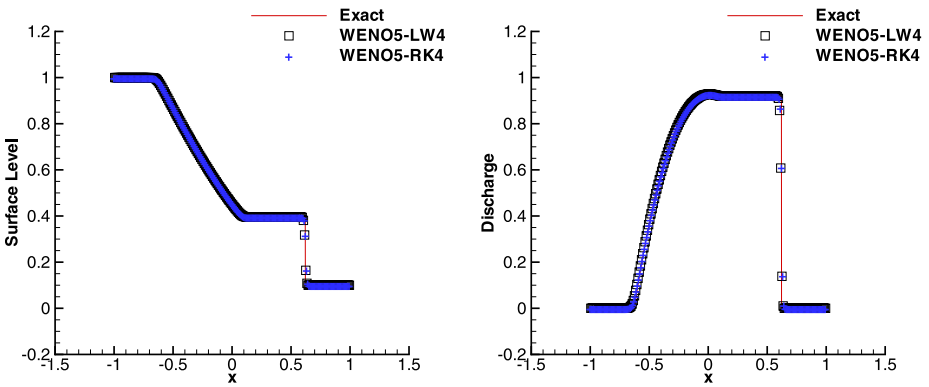


**Fig. 4** Dam break on a flat bed by WENO5-LW4 and WENO5-RK4. *Left*: surface level. *Right*: discharge

The water depth $D$ and the discharge $Du$ using the WENO5-LW3 and WENO5-RK3 schemes on a mesh with 200 points and exact solution are plotted in Fig. 3, and in Fig. 4 is by the WENO5-LW4 and WENO5-RK4 schemes, which show very good agreement with the exact solution [5], and no spurious oscillations occurred. We run 200 times as the CPU time for every program, the CPU time is 3.95 s for WENO5-LW3, 4.49 s for WENO5-RK3 schemes, and 4.39 s for WENO5-LW4, 5.82 s for WENO-RK4 schemes. We can see that the cost CPU time of WENO5-RK is about 14% more than that of WENO5-LW for this test.

*Example 3.4* A small perturbation of steady-state water. This is a classical example to show the capability of the proposed scheme for the perturbation of the stationary state [16]. In the domain $[0, 2]$, the bottom topography is given by the function

$$b(x) = \begin{cases} 0.25(\cos(10\pi(x-1.5))+1) & 1.4 \le x \le 1.6 \\ 0 & \text{otherwise} \end{cases},$$

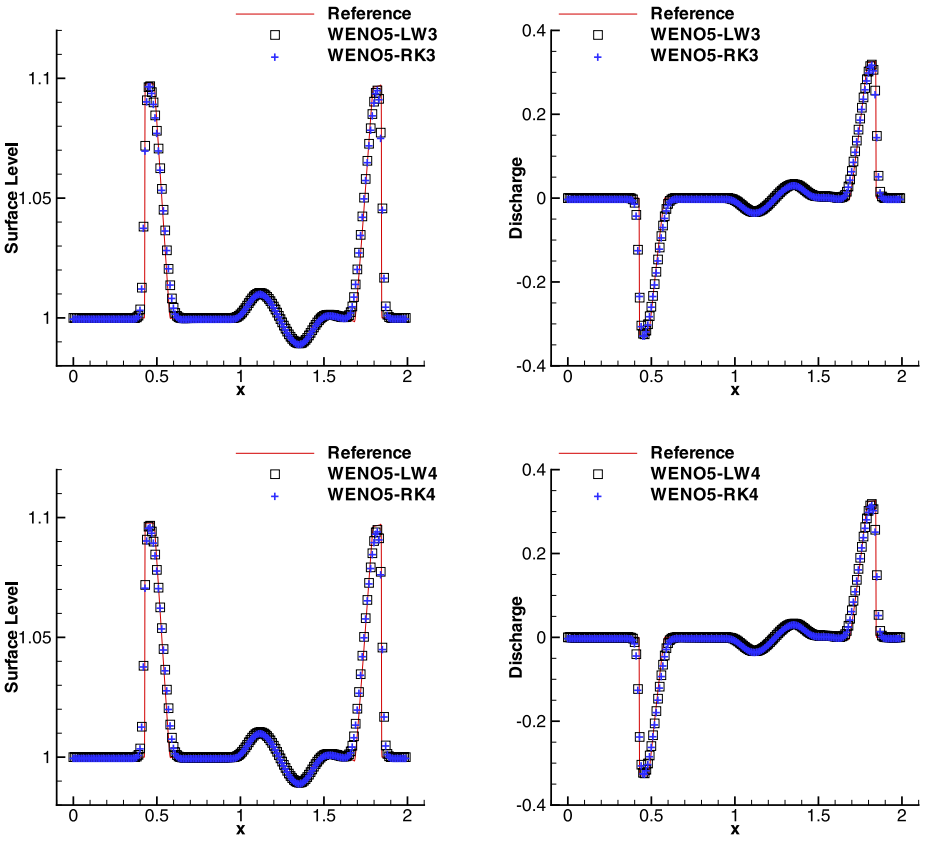


**Fig. 5** Big pulse for the small perturbation of steady-state water by WENO5-LW3, WENO5-RK3, WENO5-LW4, WENO5-RK4. *Left*: surface level. *Right*: discharge

the initial data are given by:

$$D(x,0) = \begin{cases} 1 - b(x) + \beta & 1.1 \le x \le 1.2 \\ 1 - b(x) & \text{otherwise} \end{cases}, \quad (Du)(x,0) = 0.$$

Here the pulse $\beta = 0.2$ (big pulse) or $\beta = 0.001$ (small pulse). For small pulse problem, we take $\varepsilon = 10^{-12}$ in the weight formulas for WENO schemes. Figures 5 and 6 displays the left and right-going waves for big pulse and small pulse separately. We can clearly see that there are no spurious numerical oscillations simulated by both WENO5-LW scheme and WENO5-RK scheme, and the results is comparable on resolution. We run 200 times for every program as the CPU time, to the big pulse problem, the CPU cost for WENO5-LW3 schemes is 4.20 s, while for WENO5-RK3 schemes is 7.44 s; for WENO5-LW4 schemes is 4.57 s, while for WENO5-RK4 schemes is 9.86 s. We can see that WENO5-RK cost about twice times of that of WENO5-LW scheme for this test.

*Example 3.5* Steady discontinuous flow over a parabolic hump. The purpose of the test is to study the convergence in time towards steady flows on non-flat bed involving trans-critical

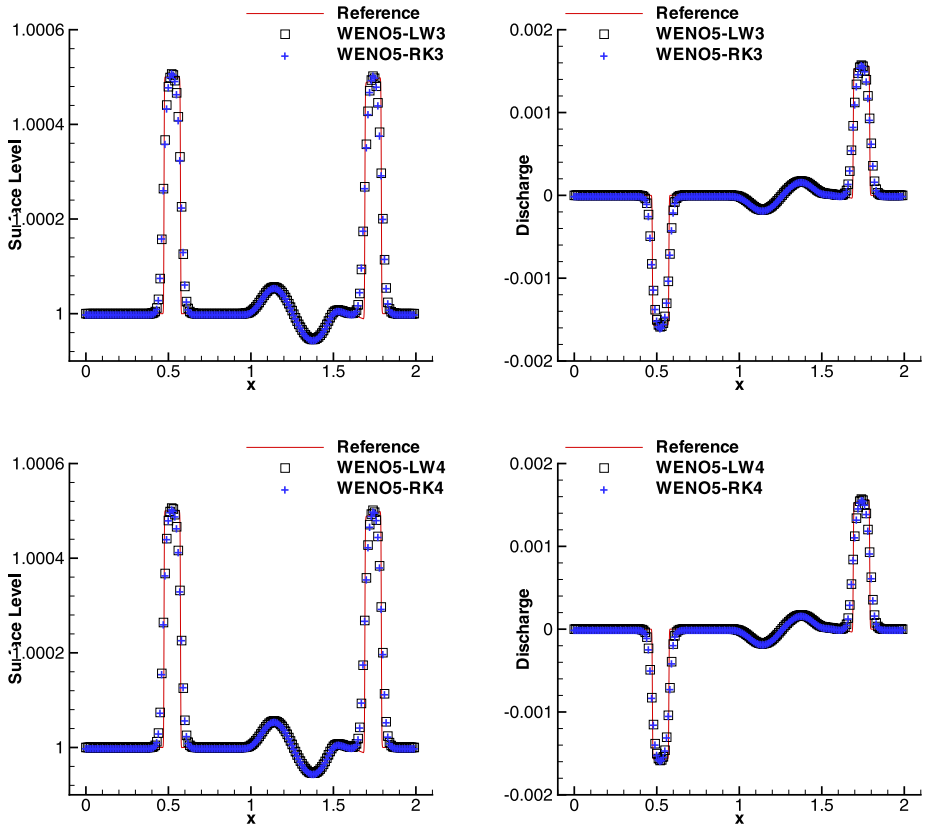


**Fig. 6** Small pulse for the small perturbation of steady-state water by WENO5-LW3, WENO5-RK3, WENO5-LW4, WENO5-RK4. *Left*: surface level. *Right*: discharge

and sub-critical flows; it is widely used to test numerical schemes for the shallow water equations, such as [4, 10].

The bottom elevation is described by the following function:

$$b(x) = \begin{cases} 0.2 - 0.05(x-10)^2 & 8 \le x \le 12 \\ 0 & \text{otherwise} \end{cases}, \tag{3.2}$$

where $x \in [0, 25]$. The initial conditions are taken as:

$$D(x,0) = 0.5 - b(x), \quad (Du)(x,0) = 0. \tag{3.3}$$

Different steady solutions can be computed involving fully sub-critical and smooth trans-critical flow and trans-critical flow with a shock. We simulate the problem until time $t =$ 200 s with three boundary conditions on mesh with 200 points. We take still water depth $h = 0.5 - b(x)$.

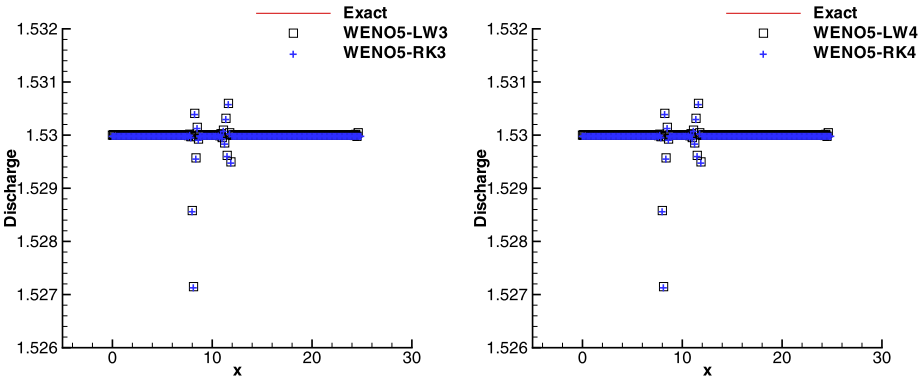


**Fig. 7** The discharge of trans-critical flow without a shock. *Left*: results by WENO5-LW3 and WENO5-RK3. *Right*: results by WENO5-LW4 and WENO5-RK4

**(a)** Trans-critical flow without a shock.

Upstream: The discharge $Du = 1.53$ m$^3$/s is imposed. Downstream: The water height $D = 0.66$ m is imposed when the flow is sub-critical. This is a transition from sub-critical to trans-critical.

The computed results of surface level $D + b$ by the WENO5-LW schemes and WENO5-RK schemes are similar and comparable to the analysis, we do not show them to save space. In Fig. 7, the computed discharge $Du$ by WENO5-LW3 schemes are plotted against that by WENO5-RK3 schemes and the exact solutions, we also plot the results of $Du$ by WENO5-LW4 and WENO5-RK4 schemes in Fig. 7. We run 20 times for every program as the CPU time, the CPU cost for WENO5-LW3 schemes is 51.13 s, while for WENO5-RK3 schemes is 93.73 s; for WENO5-LW4 schemes is 58.91 s, while for WENO5-RK4 schemes is 125.10 s. We can see that WENO5-RK cost about twice times of that of WENO5-LW scheme for this test.

**(b)** Trans-critical flow with a shock.

Upstream: The discharge $Du = 0.18$ m$^3$/s is imposed. Downstream: The water height $D = 0.33$ m is imposed. In this case, a stationary shock can appear on the surface.

The discharge $Du$ computed by WENO5-LW3 and WENO5-RK3 are plotted in Fig. 8, and also the numerical solutions obtained by WENO5-LW4 scheme and WENO4-RK4 schemes. We run 20 times for every program as the CPU time, the CPU cost for WENO5-LW3 schemes is 29.48 s, while for WENO5-RK3 schemes is 44.65 s; for WENO5-LW4 schemes is 33.28 s, while for WENO5-RK4 schemes is 59.45 s. We can see that WENO5-RK cost more than one and a half times of that of WENO5-LW scheme for this test.

**(c)** Sub-critical flow with a shock.

Upstream: The discharge $Du = 4.42$ m$^3$/s is imposed. Downstream: The water height $D = 2$ m is imposed. The imposed conditions and the bottom elevation cause the purely sub-critical flow over the whole domain.

The comparison of the discharge $Du$ using the WENO5-LW3 scheme and WENO5-RK3 schemes, WENO5-LW4 and WENO5-RK4 schemes are shown in Fig. 9. From all these results, we can see that the results using the WENO5-LW scheme are similar to these by WENO5-RK schemes, which show almost non-oscillatory results in good agreement with the analytical solution [6]. The discharges are almost accurately computed, only few

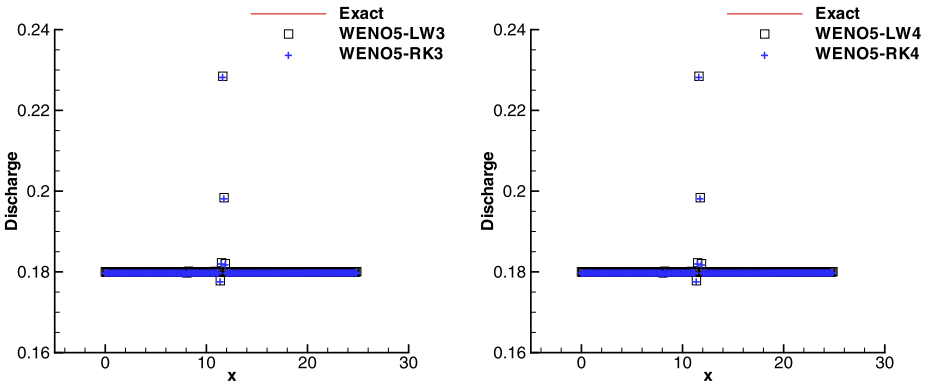


**Fig. 8** The discharge of trans-critical flow without a shock. *Left*: results by WENO5-LW3 and WENO5-RK3. *Right*: results by WENO5-LW4 and WENO5-RK4

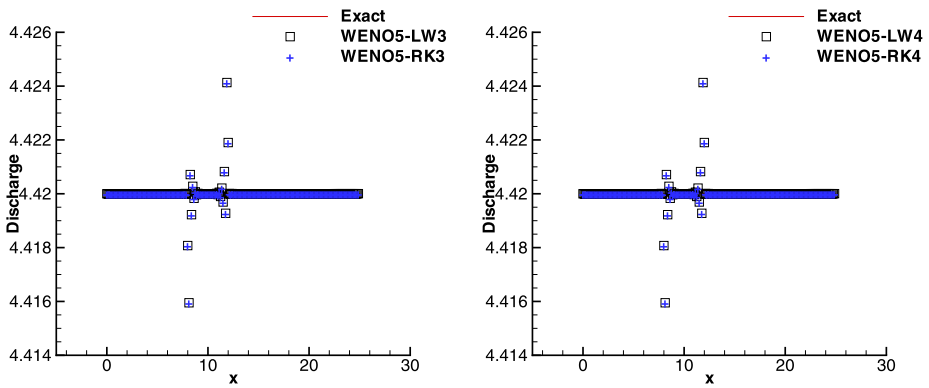


**Fig. 9** The discharge of trans-critical flow without a shock. *Left*: results by WENO5-LW3 and WENO5-RK3. *Right*: results by WENO5-LW4 and WENO5-RK4

numerical point-values of flow discharge do not agree well with the analytical solution, but these points are located at the shock position.

We run 20 times for every program as the CPU time, the CPU cost for WENO5-LW3 schemes is 64.07 s, while for WENO5-RK3 schemes is 96.88 s; for WENO5-LW4 schemes is 71.64 s, while for WENO5-RK4 schemes is 129.32 s. We can see that WENO5-RK cost more than one and a half times of that of WENO5-LW scheme for this test.

*Example 3.6* Dam breaking problem over a rectangular bump. To check the performance of shallow flows for problems over a discontinuous or big change of gradient bottom topography, we use the test as in [15, 16]. On the domain [0, 1500], the bottom topography are given by

$$b(x) = \begin{cases} 8 & |x - 750| \leq 1500/8 \\ 0 & \text{otherwise} \end{cases},$$

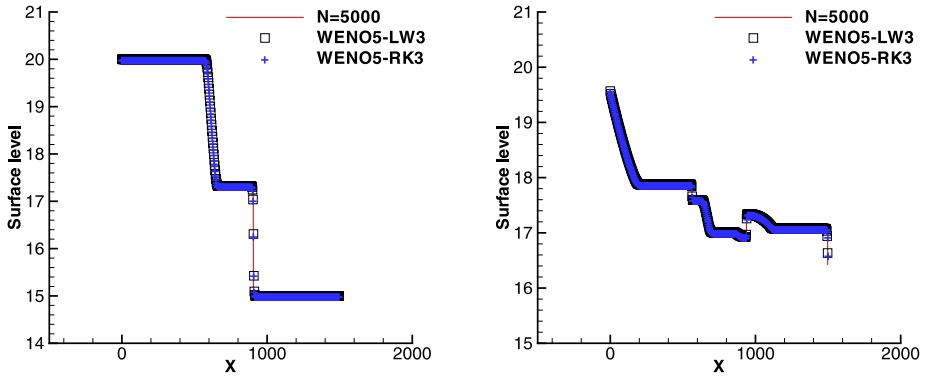


**Fig. 10** Dam breaking problem over a rectangular bump. The numerical results of surface level by WENO5-LW3 and WENO5-RK3 schemes with 500 grid points. *Left*: at time $t = 15$ s. *Right*: at time $t = 60$ s

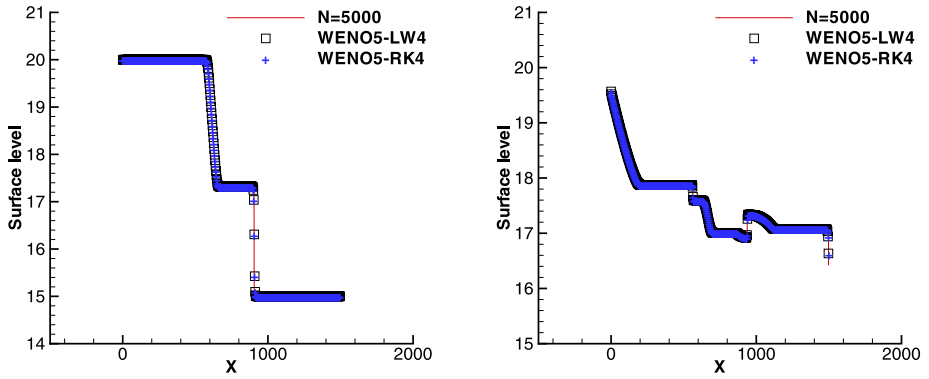


**Fig. 11** Dam breaking problem over a rectangular bump. The numerical results of surface level by WENO5-LW4 and WENO5-RK4 schemes with 500 grid points. *Left*: at time $t = 15$ s. *Right*: at time $t = 60$ s

the initial data are given by:

$$D(x,0) = \begin{cases} 20 - b(x) & x \le 750 \\ 15 - b(x) & \text{otherwise} \end{cases}, \quad (Du)(x,0) = 0.$$

In this test, we take still water height $h = 15 - b(x)$. We compute up to $t = 15$ s and $t = 60$ s separately. For the ending time $t = 15$ s, the results is similar to that of a dam break on a flat bed, because the flow have not propagate out of the rectangle. For the ending time $t = 60$ s, the water height $D(x)$ is discontinuous at the discontinuous points of bottom topography, while the surface level is smooth there. The numerical results by WENO5-LW3 schemes against with WENO5-RK3 schemes with 500 points and reference results with 5000 points are shown in Fig. 10, in Fig. 11 is results by WENO5-LW4 and WENO5-RK4 schemes.

We run 20 times as the CPU costs for the ending time $t = 60$ s, the cost CPU time is 6.18 s for WENO5-LW4, 7.33 s for WENO-RK4 schemes.

**Table 5** An two-dimensional accuracy test. $L^\infty$ errors and numerical orders of accuracy by the WENO5-LW4 scheme

| $N$ | $D$ | | $Du$ | | $Dv$ | |
|---|---|---|---|---|---|---|
| | $L^\infty$ error | order | $L^\infty$ error | order | $L^\infty$ error | order |
| $25 \times 25$ | 1.052E−1 | | 1.541E−1 | | 9.326E−1 | |
| $50 \times 50$ | 2.749E−2 | 1.94 | 2.374E−2 | 2.70 | 2.203E−1 | 2.08 |
| $100 \times 100$ | 4.404E−3 | 2.64 | 3.094E−3 | 2.94 | 3.780E−2 | 2.54 |
| $200 \times 200$ | 2.957E−4 | 3.90 | 1.843E−4 | 4.07 | 2.178E−3 | 4.12 |
| $400 \times 400$ | 1.248E−5 | 4.57 | 7.197E−6 | 4.68 | 9.294E−5 | 4.55 |

**Table 6** An two-dimensional accuracy test. $L^1$ errors and numerical orders of accuracy by the WENO5-LW4 scheme

| $N$ | $D$ | | $Du$ | | $Dv$ | |
|---|---|---|---|---|---|---|
| | $L^1$ error | order | $L^1$ error | order | $L^1$ error | order |
| $25 \times 25$ | 1.167E−2 | | 3.946E−2 | | 9.393E−2 | |
| $50 \times 50$ | 1.459E−3 | 3.00 | 2.767E−3 | 3.83 | 1.270E−2 | 2.89 |
| $100 \times 100$ | 1.084E−4 | 3.75 | 1.581E−4 | 4.13 | 9.195E−4 | 3.79 |
| $200 \times 200$ | 4.845E−6 | 4.48 | 6.786E−6 | 4.54 | 4.009E−5 | 4.52 |
| $400 \times 400$ | 1.825E−7 | 4.73 | 3.116E−7 | 4.44 | 1.477E−6 | 4.76 |

*Example 3.7* An two-dimensional accuracy test. To check the numerical order of accuracy for two-dimensional shallow water equations we use the same test as Xing and Shu [16]. On the unit square $[0, 1] \times [0, 1]$, we choose the bottom topography

$$b(x, y) = \sin(2\pi x) + \cos(2\pi y),$$

the initial data are given by:

$$D(x, y, 0) = 10 + e^{\sin(2\pi x)} \cos(2\pi y),$$

$$(Du)(x, y, 0) = \sin(\cos(2\pi x)) \sin(2\pi y),$$

$$(Dv)(x, y, 0) = \cos(2\pi x) \cos(\sin(2\pi y)).$$

We take the still water height $h$ as $h = 10 - b(x, y)$. The time step is modified as one-dimensional case in order to get fifth numerical order. We compute up to time $t = 0.05$ when there is no shocks in the solution, with 4-periodic boundary conditions. The reference solution is computed with the same scheme and 1600 points in $x$-direction and $y$-direction separately, since the exact solution is unknown.

In Table 5 and Table 6, the $L^\infty$ and $L^1$ errors and accuracy order of water depth $D$, the discharge $Du$ and $Dv$ by WENO5-LW4 scheme are displayed, $N$ is cell number. For comparison, we also give the $L^\infty$ and $L^1$ numerical error and orders by WENO5-RK4 scheme in Table 7 and Table 8. We can see that the numerical errors and orders of accuracy are similar by the WENO5-LW4 and WENO5-RK4 schemes, both schemes almost reach the designed the fifth orders.

*Example 3.8* A small perturbation of steady-state water. This is a classical example to show the capability of the proposed scheme for the perturbation of the stationary state for two-

**Table 7** An two-dimensional accuracy test. $L^\infty$ errors and numerical orders of accuracy by the WENO5-RK4 scheme

| $N$ | $D$ | | $Du$ | | $Dv$ | |
|---|---|---|---|---|---|---|
| | $L^\infty$ error | order | $L^\infty$ error | order | $L^\infty$ error | order |
| $25 \times 25$ | 9.597E−2 | | 1.446E−1 | | 1.014E−0 | |
| $50 \times 50$ | 2.507E−2 | 1.94 | 2.261E−2 | 2.68 | 2.764E−1 | 1.88 |
| $100 \times 100$ | 4.139E−3 | 2.60 | 2.692E−3 | 3.07 | 4.201E−2 | 2.72 |
| $200 \times 200$ | 3.435E−4 | 3.59 | 1.906E−4 | 3.82 | 3.229E−3 | 3.70 |
| $400 \times 400$ | 1.959E−5 | 4.13 | 1.106E−5 | 4.11 | 1.769E−4 | 4.19 |

**Table 8** An two-dimensional accuracy test. $L^1$ errors and numerical orders of accuracy by the WENO5-RK4 scheme

| $N$ | $D$ | | $Du$ | | $Dv$ | |
|---|---|---|---|---|---|---|
| | $L^1$ error | order | $L^1$ error | order | $L^1$ error | order |
| $25 \times 25$ | 1.190E−2 | | 3.730E−2 | | 9.962E−2 | |
| $50 \times 50$ | 1.428E−3 | 3.06 | 2.789E−3 | 3.74 | 1.339E−2 | 2.90 |
| $100 \times 100$ | 1.022E−4 | 3.80 | 1.554E−4 | 4.17 | 9.545E−4 | 3.81 |
| $200 \times 200$ | 5.212E−6 | 4.29 | 7.308E−6 | 4.41 | 4.803E−5 | 4.31 |
| $400 \times 400$ | 2.628E−7 | 4.31 | 3.905E−7 | 4.23 | 2.387E−6 | 4.33 |

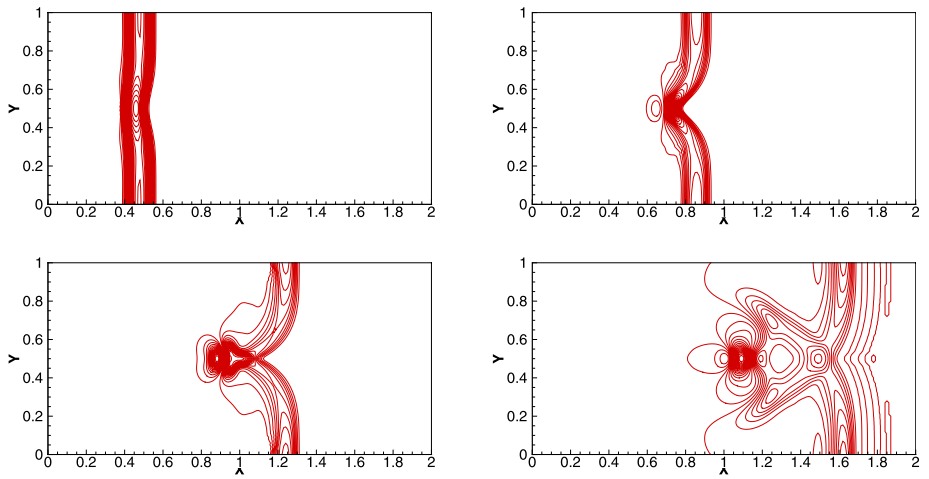


**Fig. 12** A small perturbation of steady-state water. The contours of the surface level at time 0.12 s (*top left*), 0.24 s (*top right*), 0.36 s (*bottom left*), 0.48 s (*bottom right*), 30 uniformly spaced contour lines

dimensional shallow water flows [9, 13]. The bottom topography is given by the function

$$b(x, y) = 0.8 \exp(-5(x - 0.9)^2 - 50(y - 0.5)^2), \quad x, y \in [0, 2] \times [0, 1].$$

The surface is initially given by

$$D(x, y) = \begin{cases} 1 - b(x, y) + 0.01 & 0.05 \le x \le 0.15 \\ 1 - b(x, y) & \text{otherwise} \end{cases}, \quad u(x, y, 0) = v(x, y, 0) = 0.$$

The absorbing extrapolation boundary conditions of left and right boundary are used, and the reflection boundary condition is used for up and down solid wall boundary.

We take the still water height $h$ as $h = 1 - b(x, y)$. Figure 12 displays the right-going disturbance as it propagates the hump on a mesh of $200 \times 100$ cells, the contours of the surface level $D + b$ are presented at different time. The results are agreement with other scholar's results and indicate that the scheme can resolve the complex small features of the flow very well. On the same mesh, to the different ending time 0.12 s, 0.24 s, 0.36 s, 0.48 s, the cost CPU time for WENO5-LW4 is 4.59 s, 9.22 s, 13.79 s, 18.39 s separately, while for WENO5-RK4 is 5.37 s,10.61 s, 15.93 s, 21.28 s. So the cost CPU time for WENO5-RK4 is about 15% more than that of WENO5-LW4.

## 4 Concluding Remarks

In this paper, we simulate one-dimensional and two-dimensional shallow water equations with source terms by high resolution finite difference WENO schemes and Lax-Wendroff-type time discretizations. We compare the numerical results by the schemes with that by finite difference WENO schemes using Runge-Kutta time discretizations addressing on CPU time and relevant efficiency. The numerical results show that the WENO5-LW schemes can simulate the current flow accurately and catch the stronger discontinuous in water wave, and the WENO5-LW schemes have smaller CPU costs for the same order of accuracy than that with Runge-Kutta time discretization.

## References

1. Aràndiga, F., Belda, A.M., Mulet, P.: Point-value WENO multiresolution applications to stable image compression. J. Sci. Comput. **43**, 158–182 (2009)
2. Balsara, D.S.: Divergence-free reconstruction of magnetic fields and WENO schemes for magnetohydrodynamics. J. Comput. Phys. **228**, 5040–5054 (2009)
3. Balsara, D.S., Shu, C.W.: Monotonicity preserving weighted essentially non-oscillatory schemes with increasingly high order of accuracy. J. Comput. Phys. **160**, 405–452 (2000)
4. Cai, Y., Navon, I.M.: Parallel block preconditioning techniques for the numerical simulation of the shallow water flow using finite element methods. J. Comput. Phys. **122**, 39–50 (1995)
5. Chleffi, V., Valaini, A., Zanni, A.: Finite volume method for simulating extreme flood events in natural channels. J. Hydraul. Res. **41**, 167–177 (2003)
6. Goutal, N., Maurel, F.: In: Proceedings of the Second Workshop on Dam-BreakWave Simulation. Technical Report HE-43/97/016/A. Electricité de France, Département Laboratoire National Hydraulique, Groupe Hydraulique Fluviale (1997)
7. Harten, A., Engguist, B., Osher, S., Chakravarthy, S.: Uniformly high order essentially non-oscillatory schemes, *III*. J. Comput. Phys. **71**, 231–303 (1987)
8. Jiang, G.S., Shu, C.W.: Efficient implementation of weighted ENO schemes. J. Comput. Phys. **126**, 202–228 (1996)
9. LeVeque, R.J.: Balancing source terms and flux gradients in high-resolution Godunov method: the quasi-steady wave-propagation algorithm. J. Comput. Phys. **346**, 146 (1998)
10. Liu, X.D., Osher, S., Chan, T.: Weighted essentially non-oscillatory schemes. J. Comput. Phys. **115**, 200–212 (1994)
11. Qiu, J.X., Shu, C.W.: Finite difference WENO schemes with Lax-Wendroff-type time discretizations. SIAM J. Sci. Comput. **24**, 2185–2198 (2003)
12. Ricchiuto, M., Abgrall, R., Deconinck, H.: Application of conservative residual distribution schemes to the solution of the shallow water equations on unstructured meshes. J. Comput. Phys. **222**, 287–331 (2007)
13. Rogers, B.D., Borthwick, Alistair G.L., Taylor, P.H.: Mathematical balancing of flux gradient and source terms prior to using Roe's approximate Riemann solver. J. Comput. Phys. **192**, 422–451 (2003)

14. Shu, C.W.: Essential non-oscillatory and weighted essentially non-oscillatory schemes for hyperbolic conservation laws. In: Cockburn, B., Johnson, C., Shu, C.W., Tadmor, E. (eds.) Advanced Numerical Approximation of Nonlinear Hyperbolic Equations. Lecture Notes in Mathematics, vol. 1697, pp. 325–432. Springer, Berlin (1998). A. Quarteroni (ed.)
15. Vukovic, S., Sopta, L.: ENO and WENO schemes with the exact conservation property for one-dimensional shallow water equations. J. Comput. Phys. **179**, 593–621 (2002)
16. Xing, Y.L., Shu, C.W.: High order finite difference WENO schemes with the exact conservation property for the shallow water equations. J. Comput. Phys. **208**, 206–227 (2005)
17. Zahran, Y.H.: An efficient WENO scheme for solving hyperbolic conservation laws. Appl. Math. Comput. **212**, 37–50 (2009)
18. Zhou, J.G., Causon, D.M., Mingham, C.G., Ingram, D.M.: The surface gradient method for the treatment of source terms in the shallow water equations. J. Comput. Phys. **168**, 1–25 (2001)
19. Zhu, J., Qiu, J.X.: Hermite WENO schemes and their application as limiters for Runge-Kutta discontinuous Galerkin method, III: unstructured meshes. J. Sci. Comput. **39**, 293–321 (2009)